DALTON
FULL PAPER

Crystal architecture of the cocrystalline salt $[Ru(\eta^5\text{-}C_5H_5)(\eta^6\text{-}trans\text{-}PhCH{=}CHPh)][PF_6]\cdot 0.5trans\text{-}PhCH{=}CHPh$ and the reversible order–disorder phase transition in $[Ru(\eta^5\text{-}C_5H_5)(\eta^6\text{-}C_6H_6)][PF_6]$

Fabrizia Grepioni,*[a] Gianna Cojazzi,[b] Dario Braga,*[c] Elisabeth Marseglia,[d] Laura Scaccianoce[e] and Brian F. G. Johnson*[e]

[a] *Dipartimento di Chimica, Università di Sassari, Via Vienna 2, 07100 Sassari, Italy*
[b] *Centro di Studio per la Fisica delle Macromolecole del CNR, c/o Dipartimento di Chimica G. Ciamician, Università di Bologna, Via Selmi 2, 40126 Bologna, Italy*
[c] *Dipartimento di Chimica G. Ciamician, Università di Bologna, Via Selmi 2, 40126 Bologna, Italy*
[d] *Cavendish Laboratory, University of Cambridge, Madingley Road, Cambridge, UK CB3 0HE*
[e] *Chemistry Department, University of Cambridge, Lensfield Road, Cambridge, UK CB3 4KW*

Received 26th October 1998, Accepted 8th December 1998

The crystal architecture, stability and behaviour with temperature of the hexafluorophosphate salts $[Ru(\eta^5\text{-}C_5H_5)(\eta^6\text{-arene})]^+$ (arene = benzene **1** or *trans*-stilbene **2**) have been investigated by variable temperature X-ray diffraction and differential scanning calorimetry. Compound **1** shows a reversible high temperature phase transition to a semi-disordered phase at 332 K. It is pseudo-isomorphous with $[Cr(\eta^6\text{-}C_6H_6)_2][PF_6]$ and with the room temperature form of $[M(\eta^5\text{-}C_5H_5)_2][PF_6]$ (M = Co or Fe), the latter species also undergoing reversible phase transitions. Crystalline **2** has been characterised in its cocrystallised form $[Ru(\eta^5\text{-}C_5H_5)(\eta^6\text{-}trans\text{-PhCH=CHPh})][PF_6]\cdot 0.5trans\text{-PhCH=CHPh}$. The *trans*-stilbene molecules fill in the voids formed in the packing when the small $[PF_6]^-$ anions assemble with the large and asymmetric $[Ru(\eta^5\text{-}C_5H_5)(\eta^6\text{-}trans\text{-PhCH=CHPh})]^+$ cations. The role of charge assisted $C\text{–}H^{(\delta+)}\cdots F^{(\delta-)}$ interactions is discussed.

Introduction

The use of organometallic building blocks in the engineering of crystalline materials allows us to introduce into the solid the characteristics of transition metals such as variable oxidation, spin states and ionic charges. The implications of utilising these features to prepare novel materials are enormous.[1]

We have concentrated our recent efforts on establishing a simple and transferable strategy for the construction of non-centrosymmetric crystals in which dipolar molecules or ions could be accommodated. The alignment of dipoles in a polar crystal, so that centrosymmetric pairs do not cancel each other, is one of the prerequisites for the construction of materials with potentials for efficient second harmonic generation effects.[2] In order to achieve this goal, we have devised two convergent strategies: (i) preparation of polar crystals *via* self-assembly of enantiomerically pure organic acids into three-dimensional channelled superstructures; (ii) synthesis of dipolar systems in which the ionic charge on the metal atom is coupled with π-electron delocalisation in unsaturated ligands. Strategy (i) is well developed and the results so far obtained are described in recent publications,[3] whereas this paper represents the first report along strategic line (ii). The third step, namely the combination of (i) and (ii) in order to obtain dipole alignment within chiral frameworks, is still at an embryonic stage of development.

We have prepared and structurally characterised by variable temperature X-ray diffraction and differential scanning calorimetry the hexafluorophosphate salts of $[Ru(\eta^5\text{-}C_5H_5)(\eta^6\text{-arene})]^+$ (arene = benzene **1** or *trans*-stilbene **2**). Besides its potential utilisation as a precursor in the construction of crystalline materials, compound **1** is interesting because of its close relationship with the previously studied isostructural species $[M(\eta^5\text{-}C_5H_5)_2][PF_6]$ (M = Co or Fe) and with $[Cr(\eta^6\text{-}C_6H_6)_2][PF_6]$. The cobaltocenium and ferrocenium crystals have been previously shown to undergo two phase transitions in a narrow temperature range.[4] Compound **2**, on the other hand, is interesting because it carries the π conjugated system of the *trans*-stilbene ligand η^6-co-ordinated to the Ru and represents a potential push-pull electronic system.

Experimental

All solvents were freshly distilled before use. The compounds $RuCl_3\cdot 3H_2O$, *trans*-stilbene, $Tl(C_5H_5)$ and $NaPF_6$ were purchased from Aldrich and used as provided.

Preparation of $[Ru(\eta^5\text{-}C_5H_5)(MeCN)_3][PF_6]$

This requires several steps.

(i) The synthesis of $[\{RuCl_2(\eta^6\text{-}C_6H_6)_2\}_x]$.[5] Excess of cyclohexa-1,3-diene (10 ml) was added to a solution of $RuCl_3\cdot 3H_2O$ (1 g) in EtOH (95%) and stirred under reflux for 2 h. This mixture was then cooled in ice for about 1 h and the resulting precipitate isolated by filtration to yield the polymeric $[\{RuCl_2(C_6H_6)\}_x]$ as a brown solid (yield 1.15 g, 94%).

(ii) The synthesis of $[Ru(\eta^5\text{-}C_5H_5)(C_6H_6)]Cl$. The compound $[\{RuCl_2(C_6H_6)\}_x]$ (0.5 g) was suspended in MeCN (30 ml) and stirred with $Tl(C_5H_5)$ (1.2 g) at room temperature for 3 h under N_2. The resulting precipitate of TlCl was removed by filtration through Celite and the filtrate evaporated under reduced pressure, to yield $[Ru(\eta^5\text{-}C_5H_5)](C_6H_6)Cl$ as a brown solid (yield 0.50 g, 91%).

(iii) The precipitation of $[Ru(\eta^5\text{-}C_5H_5)(C_6H_6)][PF_6]$ 1. The compound $[Ru(\eta^5\text{-}C_5H_5)(C_6H_6)]Cl$ (0.5 g) prepared according

to (ii) was dissolved in water (60 ml) to give a brown solution. The mixture was filtered to give a clear yellow solution to which $NaPF_6$ (1 g) was added. A precipitate of $[Ru(\eta^5\text{-}C_5H_5)(C_6H_6)][PF_6]$ **1** was immediately obtained. This compound was isolated by filtration as a white solid, which was dried under vacuum and recrystallised by slow evaporation from a solution in acetonitrile to give colourless single crystals (yield 0.30 g, 43%).

(iv) Synthesis of $[Ru(\eta^5\text{-}C_5H_5)(MeCN)_3][PF_6]$. The compound $[Ru(\eta^5\text{-}C_5H_5)(C_6H_6)][PF_6]$ (0.35 g) was dissolved in MeCN (180 ml) and the solution then irradiated with a 400 W Ace-Thandra Hg lamp (medium pressure) for 18 h. The resulting golden-yellow solution was evaporated under reduced pressure to afford the required product $[Ru(\eta^5\text{-}C_5H_5)(MeCN)_3][PF_6]$ as a yellow solid. This product is air stable in the solid state (yield 0.30 g, 91%).

Synthesis of $[Ru(\eta^5\text{-}C_5H_5)(\textit{trans}\text{-PhCH=CHPh})][PF_6]\cdot\textit{trans}$-PhCH=CHPh 2

The compound $[Ru(\eta^5\text{-}C_5H_5)(MeCN)_3][PF_6]$ (0.1 g) was dissolved in CH_2Cl_2 (120 ml) under N_2 and to this solution was added *trans*-stilbene (0.35 g). The mixture was stirred for 2 h at room temperature under N_2 and then refluxed for 3 h. The resulting solution was evaporated under reduced pressure to afford $[Ru(\eta^5\text{-}C_5H_5)(\textit{trans}\text{-PhCH=CHPh})][PF_6]$ as a brown solid. The product was washed several times with hexane to eliminate the excess of *trans*-stilbene. The solution of hexane and *trans*-stilbene was eliminated and the remaining solid dried under vacuum and dissolved in acetonitrile. Slow evaporation of the solvent gave rise to the formation of colourless single crystals of $[Ru(\eta^5\text{-}C_5H_5)(\textit{trans}\text{-PhCH=CHPh})][PF_6]\cdot\textit{trans}$-PhCH=CHPh **2** (yield 0.70 g, 53%).

Differential scanning calorimetry (DSC)

DSC Thermograms of compound **1** were measured on a Perkin-Elmer DSC-7 apparatus in sealed aluminium pans. Crystalline **1** (8.85 mg) was taken from the same crystal batch used for the diffraction experiments. Repeated cycles of cooling and heating (scanning rate 5.0 °C min^{-1}) showed hystereses of *ca.* 5 °C. The Form I ⟶ Form II phase transition was observed at 59.3 °C (332.45 K) whereas on cooling the exothermic peak occurred at 54.0 °C (327.15 K).

Crystal structure determination

Diffraction intensities for compounds **1** and **2** were collected on an Enraf-Nonius CAD-4 diffractometer equipped with a graphite monochromator (Mo-Kα radiation, $\lambda = 0.71069$ Å). The Oxford Cryosystem device was used for the low and high temperature data collections.

Crystal data. *Compound 1 (Form I).* $C_{11}H_{11}F_6PRu$, M = 389.24, orthorhombic, space group $Pna2_1$, a = 9.672(4), b = 9.754(4), c = 27.09(2) Å, V = 2556(2) Å^3, Z = 8, T = 273(2) K, D_c = 2.023 g cm^{-3}, μ = 1.406 mm^{-1}, 3172 reflections measured, refinement on F^2 (2794 independent reflections) for 193 parameters; $wR(F^2$, all reflections) = 0.252, $R1$ = 0.074, S = 0.994; crystal size 0.20 × 0.16 × 0.15 mm, $F(000)$ = 1520; θ range 3.0–27.0°.

Compound 1 (Form II). $C_{11}H_{11}F_6PRu$, M = 389.24, orthorhombic, space group $Pban$, a = 9.806(14), b = 9.829(13), c = 6.934(10) Å, V = 668(2) Å^3, Z = 2, T = 363(2) K, D_c = 1.934 g cm^{-3}, μ = 1.344 mm^{-1}, 721 reflections measured, refinement on F^2 (589 independent reflections) for 54 parameters; $wR(F^2$, all reflections) = 0.349, $R1$ = 0.128, S = 1.345; crystal size 0.20 × 0.16 × 0.15 mm, $F(000)$ = 380; θ range 3.0–25.0°.

Compound 2. $C_{12}H_{23}F_6PRu$, M = 581.48, monoclinic, space group $P2_1/n$, a = 11.897(6), b = 14.58(2), c = 13.549(10) Å, β = 93.38°, V = 2346(4) Å^3, Z = 4, T = 213(2) K, D_c = 1.647 g cm^{-3}, μ = 0.797 mm^{-1}, 1168 reflections measured, refinement on F^2 (3994 independent reflections) for 293 parameters; $wR(F^2$ all) = 0.119, $R1$ = 0.042, S = 1.106; crystal size 0.16 × 0.16 × 0.15 mm, $F(000)$ = 380; θ range 3.0–25.0°.

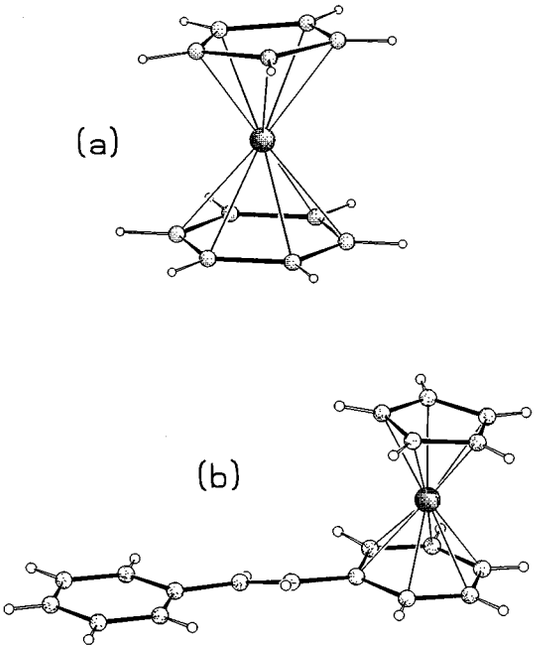

Fig. 1 Schematic representation of the cations in crystalline compounds **1** and **2**.

It should be pointed out that species like **1** and **2** do not give high quality crystals as reflected by the limited accuracy of the unit cell parameters, particularly with respect to the long cell axes. This is an unfortunate characteristic shared with all other members of the family of cationic sandwich complexes discussed in this paper.

The computer programs SHELXS 86[6a] and SHELXL 92[6b] were used for structure solution and refinement. All non-H atoms except the C atoms in compound **1** were treated anisotropically. The C_5H_5 and C_6H_6 rings in Form I of **1** were refined as rigid groups (C–C 1.42 and 1.39 Å for the two rings, respectively). Hydrogen atoms were added in calculated positions and refined riding on their respective C atoms. No attempt was made to model the H atom positions in the high temperature Form II of **1**. For all molecular representations the graphic program SCHAKAL 97[6c] was used. The program PLATON[6d] was used to calculate the hydrogen bonding interactions of the $C\text{–}H^{(\delta+)}\cdots F^{(\delta-)}$ type. For these calculations all C–H distances were normalised to the neutron derived value (1.08 Å).

CCDC reference number 186/1277.

Results and discussion

Ion organisation and phase transitions in crystalline compound 1

A schematic representation of the $[Ru(\eta^5\text{-}C_5H_5)(\eta^6\text{-}C_6H_6)]^+$ cation is shown in Fig. 1(a). Since the focus of this paper is on the supramolecular organisation of the ions in the solid state, the geometry of cation **1** will not be discussed in detail.

The crystal structure of compound **1** ought, instead, to be discussed in the light of what is known about the structures of the crystalline species $[M(\eta^5\text{-}C_5H_5)_2][PF_6]$ (M = Co or Fe) and $[Cr(\eta^6\text{-}C_6H_6)_2][PF_6]$ because of the analogy in packing arrangement and in phase transitional behaviour. Indeed, crystalline $[M(\eta^5\text{-}C_5H_5)_2][PF_6]$ (M = Co or Fe) are remarkable structural systems since both crystals are able to *switch* reversibly between three phases, two of which are fully ordered.[4] The intermediate phase (called Form I) that is obtained by crystallisation at room temperature is stable towards phase transition within an interval of *ca.* 75 °C in the case of the cobalt salt and

Table 1 Comparison of cell parameters and packing coefficient values for compound **1** and the $[M(C_5H_5)_2]^+$ (M = Co or Fe) and $[Cr(C_6H_6)_2]^+$ hexafluorophosphate salts

Species	T/K	Form	a/Å	b/Å	c/Å	β/°	V_{cell}/Å^3	p.c.
1	100	I	9.517(3)	9.666(8)	26.430(9)	—	2431(2)	0.70
	223	I	9.648(6)	9.762(5)	26.959(11)	—	2539(2)	0.67
	273	I	9.672(4)	9.754(4)	27.09(2)	—	2556(2)	0.67
	363	II	9.806(14)	9.829(13)	6.934(10)	—	668(2)	0.64
Co [4b]	243	II	13.419(7)	9.286(5)	9.343(6)	96.17(6)	1157(1)	0.69
Co [4b]	293	I	13.355(3)	9.441(8)	9.427(6)	92.87(4)	1187(1)	0.67
Co [4b]	323	III monoclinic [a]	13.426(5)	9.518(5)	9.505(5)	90.17(4)	1215(1)	0.65
Fe [7c]	143	II	13.431(9)	9.268(4)	9.328(6)	96.91(6)	1153(1)	0.70
Fe [7c]	299	I	13.408(6)	9.530(2)	9.482(2)	93.17(3)	1209(1)	0.67
Fe [4b]	360	III	6.806(4)	—	—	—	315.3(3)	0.64
Cr [4b]	203	—	9.587(6)	9.661(4)	27.510(10)	—	2548(2)	0.70
Cr [4b]	293	—	9.667(8)	9.712(4)	27.74(2)	—	2604(3)	0.69

[a] The high temperature phase can also be described in a cubic system with a = 6.72(1) Å.[4b]

of 134 °C in the case of Fe.[7] In the case of Co, which has been studied in greater detail, the whole phase transitional behaviour has been described as a progressive 'adjustment' of the crystal structure to the dynamic requirements of the globular cations which need more space as the temperature increases. The phase transitions were followed by DSC and by variable temperature single crystal diffraction.[4,7] Structural parameters concerning the four crystals are summarised in Table 1.

The structure of the metallocenium (M = Fe or Co) is related to that of the bis(benzene)chromium analogue, $[Cr(\eta^6\text{-}C_6H_6)_2][PF_6]$. In spite of the difference in molecular structure, the chromium salt crystallises in a manner which is strictly related to that of the low temperature phases of Co and Fe, and does not undergo phase changes on cooling. Topologically, the structure of the cation $[Ru(\eta^5\text{-}C_5H_5)(\eta^6\text{-}C_6H_6)]^+$ **1** is intermediate between those of the bis(cyclopentadienyl) and the bis(benzene) sandwiches.

Table 1 allows a comparison of the packing coefficients (p.c.), *i.e.* of the efficiency of volume occupation,† in the various forms of $[M(\eta^5\text{-}C_5H_5)_2][PF_6]$ (M = Co or Fe) and $[Cr(\eta^6\text{-}C_6H_6)_2][PF_6]$ with that of $[Ru(\eta^5\text{-}C_5H_5)(\eta^6\text{-}C_6H_6)][PF_6]$ **1**. It is worth noting that the p.c. values vary from 0.69 to 0.65 and from 0.70 to 0.64, on going from low to high temperature, for Co and Fe respectively. These changes reflect a substantial decrease of the crystal density as the temperature is raised in keeping with the 'plasticity' of the systems. In the case of $[Ru(\eta^5\text{-}C_5H_5)(\eta^6\text{-}C_6H_6)][PF_6]$ the p.c. values change analogously, going from 0.70 to 0.64. On the contrary, the crystalline chromium complex, which retains the same packing arrangement over the entire temperature range, undergoes a much smaller p.c. change with temperature (from 0.70 to 0.69).

In terms of ion organisation all these crystal structures show an almost identical distribution in space of the anions and cations in spite of the differences in space groups and unit cell axes. In all structures there are two 'types' of cations: those lying in plane with axes at *ca*. 90° (cations **A**, see Fig. 2) and those 'oblique' over the plane (cations **B**). In all structures the PF_6^- anions ideally occupy the corners of a nearly cubic 'box' in which the cations are encapsulated.

Differences between the crystals listed in Table 1 arise from the relative orientation of the two types of cations (see Scheme 1). In compound **1**, as well as in the room temperature phase of cobalt and iron salts, the cations **B** are 'eclipsed' in projection onto cations of type **A** (see also Fig. 3). In the cobalt and iron

† Packing coefficients are obtained from $(V_{anion} + V_{cation})Z/V_{cell}$ where Z is the number of formulae in the unit cell, V_{cell} the cell volume and V_{anion} and V_{cation} are the volumes of the anions and cations evaluated by the integration method.[8]

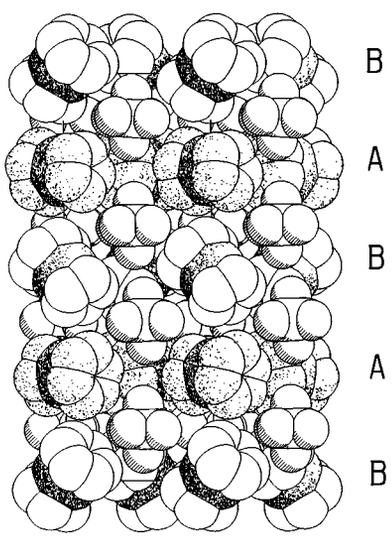

Fig. 2 The ion organisation in crystalline compound **1** (Form I); view down the *a* axis. There are two 'types' of cations: those lying in plane with axes at *ca.* 90° (cations **A**) and those 'oblique' over the plane (cations **B**) (see also Scheme 1). The PF_6^- anions occupy the interstices and ideally define the corners of a nearly cubic box in which the cations are encapsulated; H atoms omitted for clarity.

low temperature phases as well as in the bis(benzene)chromium salt cations **A** and **B** are instead staggered, *i.e.* the cation axes are, in projection, at *ca*. 90°. The second relevant difference is in the sequence of cations **B** along the cell axis. For Co and Fe they have the same orientation; in the chromium species the periodicity is doubled and the cations **B** alternate in zigzag fashion.

To summarise this analysis, the structure of compound **1** can be seen as being intermediate between that of the bis(benzene) complex (same zigzag of cations **B**, same periodicity) and that of the room temperature bis(cyclopentadienyl) complexes (cations **A** and **B** eclipsed).

High temperature phase of crystalline compound 1

Crystalline compound **1** does not undergo a low-temperature phase transition on decreasing the temperature to 223 K on the DSC and to 100 K on the diffractometer, while it shows an order–disorder phase transition on increasing the temperature. The DSC thermogram is shown in Fig. 4. On heating, the endothermic peak occurs at 59.3 °C (332.5 K), whereas on cooling the exothermic peak occurs at 54.0 °C (327.2 K). The high temperature phase is named Form II. The presence of the thermal

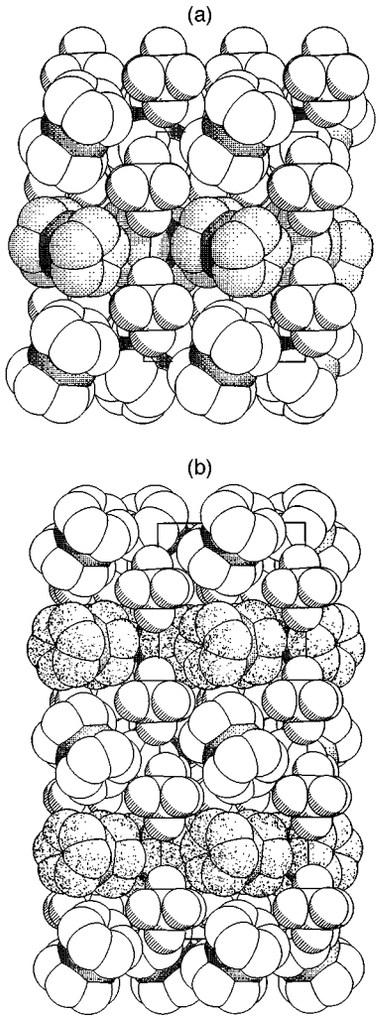

Fig. 3 The ion organisation in the metallocenium salts $[M(\eta^5\text{-}C_5H_5)_2][PF_6]$ (M = Co or Fe, Form I) (a) and $[Cr(\eta^6\text{-}C_6H_6)_2][PF_6]$ (b). Note how the distribution of ions for **1** (Fig. 2) is intermediate between those in (a) and (b); H atoms omitted for clarity.

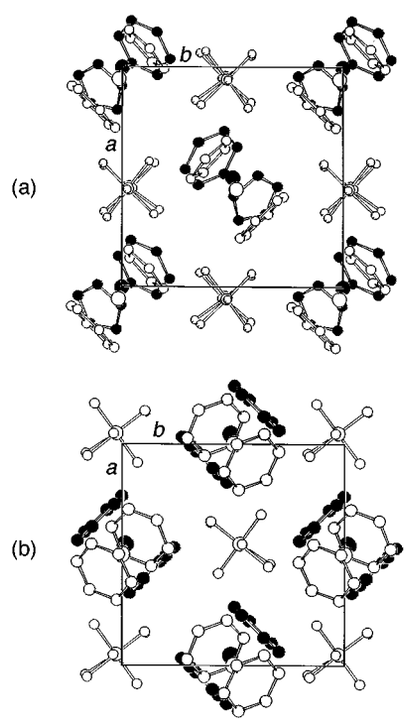

Scheme 1

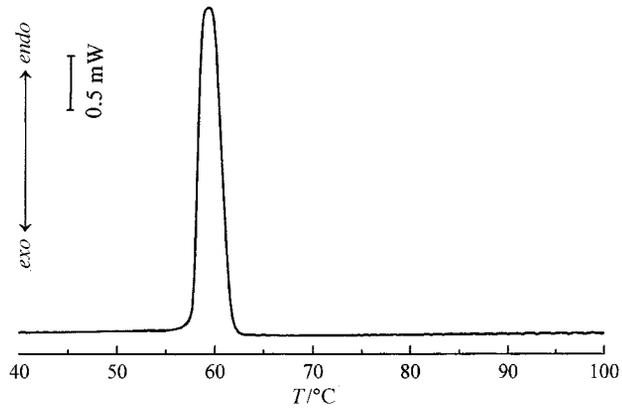

Fig. 4 DSC Thermogram showing the phase transition in compound **1**.

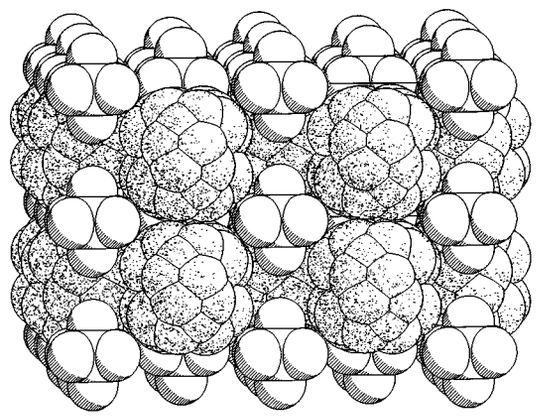

Fig. 5 Space-filling projection in the *bc* plane of the high temperature Form II of crystalline compound **1**.

hysteresis is not surprising and has been observed also in the case of Co and Fe. The enthalpy difference associated with the transition is 4.16 kJ mol^{-1}, which is comparable with the values obtained from the DSC measurements for the order–disorder phase transitions in $[M(\eta^5\text{-}C_5H_5)_2][PF_6]$ (3.05 kJ mol^{-1} for M = Co, 4.50 kJ mol^{-1} for M = Fe).

As in the case of the cobalt salt, we have been able to collect diffraction data at a high temperature (363 K). The phase transition has been followed on the single crystal diffractometer. Obviously, the high temperature data set of compound **1** is affected by a severe loss of diffraction power. Only a few hundred reflections are measurable at 363 K and the limited number of reflections reduces the resolution, which is a serious drawback in the presence of disorder. Nonetheless, we have been able to locate peaks in the Fourier maps that correspond to the fraction of carbon atoms with site occupancy in the range 0.20–0.60. A space-filling projection of Form II in the high temperature settings is shown in Fig. 5. It can easily be appreciated how the ordered distribution of the anions is retained in the high-temperature phase whereas the cations show orientational disorder in the sites. The crystal appears to behave as a semi-plastic system, in which local order is lost (but only as far as the cations are concerned) whereas long range order, *i.e.* translational symmetry, is maintained. The most remarkable aspect of this structure, as in the cases of $[M(\eta^5\text{-}C_5H_5)_2][PF_6]$ (M = Co or Fe) discussed previously, is the fact that the ordered distribution of cations and anions observed in the room temperature experimental structure is fully restored on cooling the crystal. Since the high temperature phase shows degenerate orientations of the cations there is no clear reason why, on returning to room temperature, such degeneracy is lost, *i.e.* order is restored. Of course, this information is not contained in the experimental diffraction data on the two systems:

they represent thermodynamic minima and there is no way to extract information on the mechanism of the phase transition. The most sensible rationale of the phenomenon is the same as the one put forward for $[M(\eta^5\text{-}C_5H_5)_2][PF_6]$ (M = Co or Fe): the high temperature phase, characterised by a cell volume four times smaller than the volume at room temperature, is the result of an average over time and space of domains that retain the original orthorhombic $Pna2_1$ structure, though with disordered cations.

Cocrystallisation of compound 2 with *trans*-stilbene and the molecular and crystal structure of 2

As mentioned in the Introduction, cation **2** carries the *trans*-stilbene ligand bound in η^6 fashion to the ruthenium centre, as schematically shown in Fig. 1(b); **2** is therefore isoelectronic with **1**. Crystal **2** is obtained from the cocrystallisation of one *trans*-stilbene molecule for every two cations and anions. The reason for the cocrystallisation is apparent (see below).

In terms of crystal packing there are two fundamental features to be described. The cations form centrosymmetric interlocked dimeric units [see Fig. 6(a)] with the 'free' benzene on the *trans*-stilbene ligand at a graphitic distance (3.3 Å) from the cyclopentadienyl ligand of the second cation. Incidentally, this kind of arrangement should actually be avoided if the dipolar characteristics of the cation were to be exploited (see Introduction). The dication units are then arranged in planes [Fig. 6(a)] which optimise surface coverage and, therefore, achieve high density within the cation layer. One may think that this efficient distribution of cations would not lead to a stable crystal because the small PF_6^- anions would not fill the space in between layers efficiently. Here is where the *trans*-stilbene 'filler' becomes useful. Fig. 6(b) shows the space filling diagram of the layer formed by the PF_6^- anions and by the *trans*-stilbene molecules. The *trans*-stilbene molecules fit conveniently into the packing of the anions and provide the necessary stability to the anionic layer. The stacking of cationic and anionic/*trans*-stilbene layers generates the crystal structure of **2** shown in Fig. 6(c). Attempts to isolate **2** in the absence of free stilbene have so far failed to give crystals suitable for single crystal X-ray diffraction.

The presence of $C\text{–}H^{(\delta+)}\cdots F^{(\delta-)}$ interactions between the cyclopentadienyl or benzene ligands and the PF_6^- anions in the hexafluorophosphate salts has been studied previously[4] and discussed in comparison with data on organic crystals.[9] We have shown that, in the case of the metallocenium (M = Fe or Co) and of the chromium complex, the length and number of short distances correlates with the position of the metal atom in the Periodic Table, *i.e.* more numerous and shorter $C\text{–}H^{(\delta+)}\cdots F^{(\delta-)}$ distances are in the order $[Cr(C_6H_6)_2]^+ > [Fe(C_5H_5)_2]^+ > [Co(C_5H_5)_2]^+$ which is also the order of increasing need of back donation from the metal atoms onto the ligands. Compounds **1** and **2** fit well into this scheme (see Table 2). Although great care should be exerted in relating distances to the energy of interaction[10] this observation strengthens the idea that the difference in charge between donor and acceptor increases the efficiency of the interaction.[11]

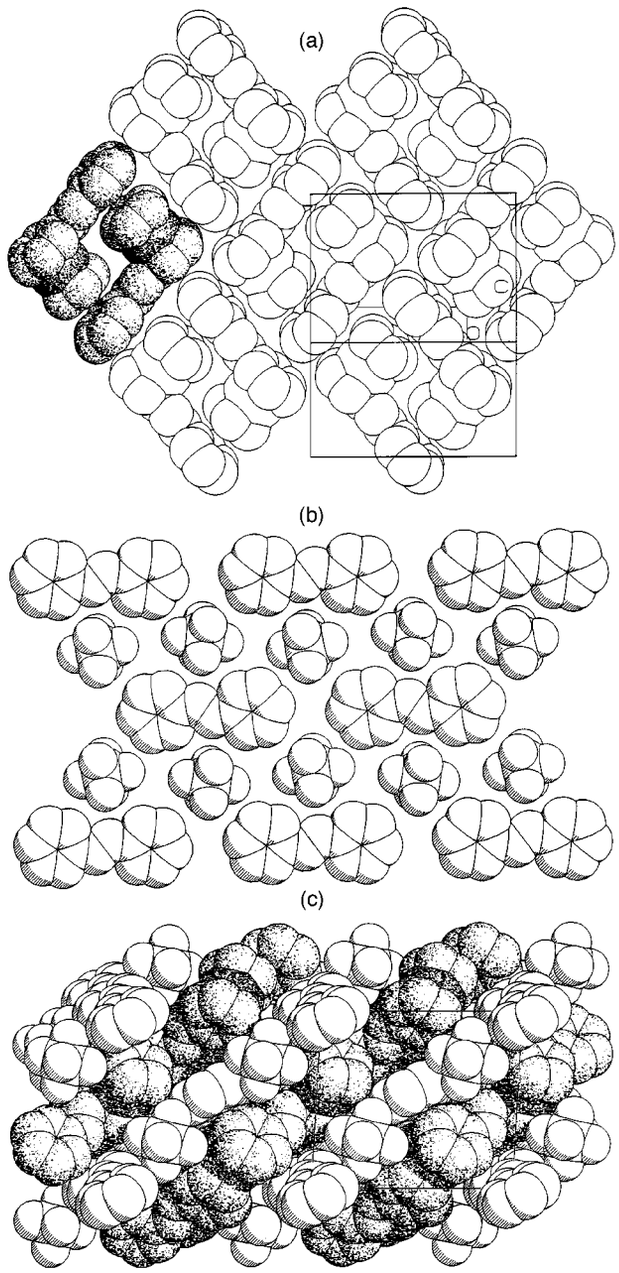

Fig. 6 (a) Space filling representation of the centrosymmetric dimeric units formed by cations in crystalline compound **2**. Note also that the dimers are arranged in planes which optimise surface coverage. (b) Space filling representation of the layer formed by the PF_6^- anions and by the *trans*-stilbene molecules. Note how the *trans*-stilbene molecules nicely fit between the anions and provide the necessary density to cover the cation layers. (c) The stacking of cationic and anionic layers; H atoms omitted for clarity.

Conclusion

With this paper we have added one more partner to the already rich family[12] of hexafluorophosphate organometallic salts that show dynamic behaviour in the solid state. The fundamental packing organisation based on the presence of two differently oriented organometallic cations encapsulated in nearly cubic 'boxes' delimited by the PF_6^- counter ions is maintained on changing the metal (Fe, Co, Ru and Cr) and/or the unsaturated carbocyclic ligand (cyclopentadienyl, benzene). All these crystals show a profusion of $C\text{–}H^{(\delta+)}\cdots F^{(\delta-)}$ interactions which have $H\cdots F$ distances appreciably shorter than the corresponding contacts present in neutral molecules and in organic fluorine compounds.[9] Since the hydrogen bond is basically electrostatic in nature, all factors influencing the charge distribution on the donor/acceptor system affect the strength of the hydrogen bond, and are clearly observed in the present case.

Compound **2**, on the other hand, demonstrates the importance of the 'shape factor' in crystal packing, *i.e.* in the supramolecular aggregation of ions and molecules in the solid state. The anisotropic shape of the $[Ru(\eta^5\text{-}C_5H_5)(\eta^6\text{-}trans\text{-}PhCH{=}CHPh)]^+$ cations leads to cation–cation aggregation (dimer formation). Though expectedly unfavoured electrostatically, the reverse (centrosymmetric) assembly of the cations optimises the available space. Thus, cocrystallisation of an extra *trans*-stilbene molecule is required to fill in space around the small PF_6^- counter ions. This is an interesting solution to the problem

Table 2 Comparison of C–H · · · F distances (H · · · F < 2.6 Å) in crystalline compounds **1** and **2**

Compound	Fragment	(C)H · · · F/Å	C(H) · · · F/Å	C–H · · · F/°
1 (Form I)	η^5-C_5H_5	2.304, 2.476, 2.541, 2.537, 2.597, 2.459, 2.571	3.108, 3.498, 3.537, 3.391, 3.323, 3.487, 3.515	129.72, 157.48, 153.02, 135.28, 123.94, 158.55, 145.52
	η^6-C_6H_6	2.558, 2.298, 2.346, 2.411, 2.503, 2.581, 2.576, 2.489, 2.243	3.339, 3.188, 3.161, 3.218, 3.219, 3.291, 3.590, 3.336, 3.277	128.55, 138.53, 131.04, 130.46, 122.76, 122.59, 156.00, 134.50, 159.66
2	η^5-C_5H_5	2.474, 2.253	3.492, 3.256	156.64, 153.61
	η^6-*trans*-Stilbene	2.513, 2.521	3.334, 3.516	132.00, 152.78
	Free stilbene	2.512	3.563	164.05

of attaining close packing but is also an undesired result if one is seeking exactly the opposite, namely predefined mono-directional orientation of the dipole moments. This may be achieved, though, if the dipoles are oriented within a chiral superstructure.[13]

Acknowledgements

Financial support from the University of Bologna Project "*Innovative Materials*" and from Ministero dell'Università e della Ricerca Scientifica e Tecnologica Project "*Supramolecular Devices*" (D. B. and F. G.) is acknowledged. D. B., F. G. and E. M. thank CRUI (Conferenza dei Rettori delle Università Italiane) and the British Council for a bilateral exchange project. D. B. and F. G. thank RSC for *International Authors grants*. B. F. G. J. and L. S. thank the EU TMR (Training, Research and Mobility) for support.

References

1 D. Braga and F. Grepioni, *Chem. Commun.*, 1996, 571; D. Braga, F. Grepioni and G. R. Desiraju, *Chem. Rev.*, 1998, **98**, 1375.
2 D. J. Williams, *Angew. Chem.*, *Int. Ed. Engl.*, 1984, **23**, 690; N. J. Long, *Angew. Chem.*, *Int. Ed. Engl.*, 1995, **34**, 21; S. R. Marder, *Inorg. Mater.*, 1992, 115.
3 D. Braga, A. L. Costa, F. Grepioni, L. Scaccianoce and E. Tagliavini, *Organometallics*, 1996, **15**, 1084; *Organometallics*, 1997, **16**, 2070; D. Braga, A. Angeloni, F. Grepioni and E. Tagliavini, *Chem. Commun.*, 1997, 1447; D. Braga and F. Grepioni, *Chem. Commun.*, 1998, 911; D. Braga, F. Grepioni and L. Maini, *Angew. Chem.*, *Int. Ed. Engl.*, 1998, **37**, 2240.
4 (*a*) D. Braga, L. Scaccianoce, F. Grepioni and S. M. Draper, *Organometallics*, 1996, **15**, 4675; (*b*) F. Grepioni, G. Cojazzi, S. M. Draper, N. Scully and D. Braga, *Organometallics*, 1998, **17**, 296; (*c*) D. Braga and F. Grepioni, in *Current Challenges on Large Supramolecular Assemblies*, ed. G. Tsoucaris, Kluwer, Dordrecht, 1998.
5 D. Catheline and D. Astruc, *J. Organomet. Chem.*, 1982, **C52**, 226.
6 (*a*) SHELXS 86, G. M. Sheldrick, *Acta Crystallogr.*, *Sect. A*, 1990, **46**, 467; (*b*) SHELX 92, G. M. Sheldrick, Program for Crystal Structure Determination, University of Göttingen, 1992; (*c*) SCHAKAL 97, E. Keller, Graphical Representation of Molecular Models, University of Freiburg, 1997; (*d*) PLATON, A. L. Spek, *Acta Crystallogr.*, *Sect. A*, 1990, **46**, C31.
7 R. Martinez and A. Tiripicchio, *Acta Crystallogr.*, *Sect. C*, 1990, **46**, 202; R. J. Webb, M. D. Lowery, Y. Shiomi, M. Sorai, R. J. Wittebort and D. N. Hendrickson, *Inorg. Chem.*, 1992, **31**, 5211; M. Sorai and Y. Shiomi, *Thermochim. Acta*, 1986, **109**, 29.
8 A. Gavezzotti, *J. Am. Chem. Soc.*, 1983, **95**, 5220.
9 J. Dunitz and R. Taylor, *Chem. Eur. J.*, 1997, **3**, 89.
10 D. Braga, F. Grepioni, Tagliavini, J. J. Novoa and F. Mota, *New J. Chem.*, 1998, 755; D. Braga, F. Grepioni and J. J. Novoa, *Chem. Commun.*, 1998, 1959.
11 D. Braga and F. Grepioni, *New. J. Chem.*, 1998, 1159.
12 See, for example: B. W. Fitzsimmons and I. Sayer, *J. Chem. Soc.*, *Dalton Trans.*, 1991, 2907; B. W. Fitzsimmons and W. G. Marshall, *J. Chem. Soc.*, *Dalton Trans.*, 1992, 73.
13 D. Braga and F. Grepioni, *J. Chem. Soc.*, *Dalton Trans.*, 1999, 1.

Paper 8/08278B